NASA TECHNICAL NOTE

NASA TN D-1683

N63 23123

NASA TN D-1683

FLIGHT VIBRATION DATA FROM THE DELTA 9 LAUNCH VEHICLE

by Lloyd A. Williams
Goddard Space Flight Center
Greenbelt, Maryland

NATIONAL AERONAUTICS AND SPACE ADMINISTRATION • WASHINGTON, D. C. • OCTOBER 1963

28

TECHNICAL NOTE D-1683

FLIGHT VIBRATION DATA FROM THE DELTA 9 LAUNCH VEHICLE

By Lloyd A. Williams

National A and S Adm.
Goddard Space Flight Center,
Greenbelt, M~~aryland~~d.

NATIONAL AERONAUTICS AND SPACE ADMINISTRATION

TECHNICAL NOTE D-1683

FLIGHT VIBRATION DATA FROM THE DELTA 9 LAUNCH VEHICLE

By Lloyd A. Williams

Goddard Space Flight Center
Greenbelt, Maryland

NATIONAL AERONAUTICS AND SPACE ADMINISTRATION

FLIGHT VIBRATION DATA FROM THE DELTA 9 LAUNCH VEHICLE

by
Lloyd A. Williams
Goddard Space Flight Center

SUMMARY

23123

Three channels of vibration data were obtained during the flight of the Delta 9 vehicle which was used to place the UK-1 satellite Ariel I (1962 o1) into earth orbit on April 26, 1962, from Cape Canaveral.

Vibration data for the three principal axes of the payload support structure were obtained from liftoff through third-stage motor burnout. Maximum vibration levels during first- and second-stage burning occurred at liftoff, staging, and fairing jettison with low levels between events. The maximum composite vibration levels for first- and second-stage burning were 2.5 g peak and 1.9 g peak for the thrust and lateral axes, respectively, and occurred at liftoff.

The third-stage motor exhibited the normal resonant burning characteristics for this type of motor, that is, the tangential and longitudinal modes caused by acoustical cavity resonances. However, since this phenomenon is already well documented, the primary purpose of this vibration experiment was to record low-frequency high-stress amplitude vibration. Consequently, the measuring systems were set up to measure low-level first- and second-stage modal vibrations. Most of the third-stage data are not realistic since the amplifiers were overloaded.

Shock transients occurred at times of premature despin. Despin of the third-stage motor and payload was scheduled to start 15 minutes after closure of the third-stage motor pressure switch; however, the first despin sequence started 1 minute and 40 seconds after the switch closed.

AUTHOR

CONTENTS

Summary i

INTRODUCTION 1

DESCRIPTION OF THE VEHICLE 1

INSTRUMENTATION 2

DATA REDUCTION 5

RESULTS 5

DISCUSSION 17

References 20

FLIGHT VIBRATION DATA FROM THE DELTA 9 LAUNCH VEHICLE

by

Lloyd A. Williams

Goddard Space Flight Center

INTRODUCTION

A continuous long-term program which will increase confidence in laboratory environmental testing is in operation at Goddard Space Flight Center. Part of this program involves the acquisition of flight vibration data to give adequate definition to laboratory test criteria, since laboratory tests are required to demonstrate the ability of the payload to withstand the vibrations encountered during launch and flight.

Since measurements of vibrations at the thrust flange of a Thor-Delta vehicle's third-stage motor during flight are virtually non-existent, and since space and weight were available on the Delta 9 vehicle which launched the UK-1 satellite Ariel I (1962 o1) from Cape Canaveral on April 26, 1962, an experiment was placed aboard the Delta 9 to help provide data for future environmental simulation of this three-stage vehicle. This report presents the results of this in-flight experiment. The Delta 9 launch vehicle placed the Ariel I satellite in an elliptical orbit at a height ranging from 210.4 nautical miles at perigee to 655.4 nautical miles at apogee.

Located between the satellite's separation system and the Delta 9 third-stage motor was a cylindrical extension called "The Dutchman." The Dutchman housed the Goddard vibration experiment, the United Kingdom solar aspect sensor, and a United Kingdom contamination sensor.

The vibration experiment telemetered three channels of data from liftoff to beyond premature despin of the Delta 9 launch vehicle. The three channels measured the vibrations along three orthogonal axes of the vehicle (longitudinal, lateral, and lateral plus 90-degrees). Telemetered data were received from Atlantic Missile Range stations Tel 2, Tel 3, Grand Bahama Island, Antigua, Whisky (downrange ship), and Hanger AE. First- and second-stage motor vibrations were monitored at Tel 2, Tel 3, Grand Bahama Island, and Hanger AE. Third-stage vibrations and premature despin transients were recorded at Antigua.

DESCRIPTION OF THE VEHICLE

Figure 1 shows the Delta 9 vehicle on its launch pad at Cape Canaveral. The description given here is extracted from Reference 1.

The first stage of the Delta 9 vehicle was a DM-18A Thor missile (320) modified to a DM-19 configuration by removal of the retro rockets, ACSP guidance system, one "engine control" pressure bottle, and nose cone. Further modifications consisted of the addition of : (1) a command destruction system, (2) an Azusa transponder tracking aid, (3) a PDM/FM 30 × 30 telemeter, (4) special circuitry to accomplish a second-stage ignition, (5) a series-parallel arrangement of four fuel-injector-pressure switches to provide the main engine cutoff signal, (6) a pressure diaphragm, and (7) a Teflon exterior insulation applied to the leading edge of the fins. The main engine was an MB-3 Block I (S/N 4312) using RP-1 and liquid oxygen as propellants.

The second stage consisted of an Aerojet-General liquid propellant propulsion system AJ10-118-009, equipment and guidance compartment, and the third-stage/payload spin table. The equipment and guidance compartment housed the Bell Telephone Laboratory guidance system, flight control system, electrical power system, flight termination system, and a PDM/FM telemeter. An externally mounted gaseous nitrogen retro system was employed to provide the required separation distance between the second and third stage at third-stage ignition. The oxidizer probes were provided as a backup engine cutoff source. Two 2KS-40 spin rockets and one 0.6KS-40 spin rocket were employed to attain the required spin rate. A C-band radar beacon was employed for vehicle tracking.

The third stage consisted of an ABL X248-A5DM (SV-186) solid propellant motor; the Dutchman; a separation system; and the UK-1 satellite. A low-drag fairing was used to protect the satellite from aerodynamic heating while flying through the sensible atmosphere. This fairing had thermal protection added to both its interior and exterior in the form of Armalon liner and Thermo-Lag, respectively. The pyrotechnic ignition of the third-stage motor was accomplished by a system employing a 15.5 ± 0.7 second delay. Because of the sensitivity of the Ariel I to contamination by motor outgassing, the dome and cylindrical portion of the third-stage motor were wrapped with aluminum foil.

INSTRUMENTATION

Three piezoelectric crystal accelerometers were secured to aluminum blocks which were bolted and cemented to the base flange of the Dutchman. The three accelerometer locations are shown on Figures 2, 3, and 4.

Signals from the accelerometers were conditioned using "charge" amplifiers and filter-clipper-bias units. The conditioned signals were then fed into an FM/FM telemeter and transmitted to ground stations via quadraloop antennas. Figure 5 is a block diagram of the instrumentation system and Figure 6 shows the instrumentation installed in the Dutchman.

The IRIG letter channels E, C, and A (15 percent deviation) were used in the FM/FM system. Thrust axis vibrations were measured on Channel E, the lateral axis vibrations were measured on Channel C, and the lateral plus 90-degree axis vibrations were measured on Channel A. These three channels had been broadbanded beyond IRIG specifications by filtering the charge amplifier outputs with low-rolloff RC low-pass filters. By this method, the frequency response of the channels was

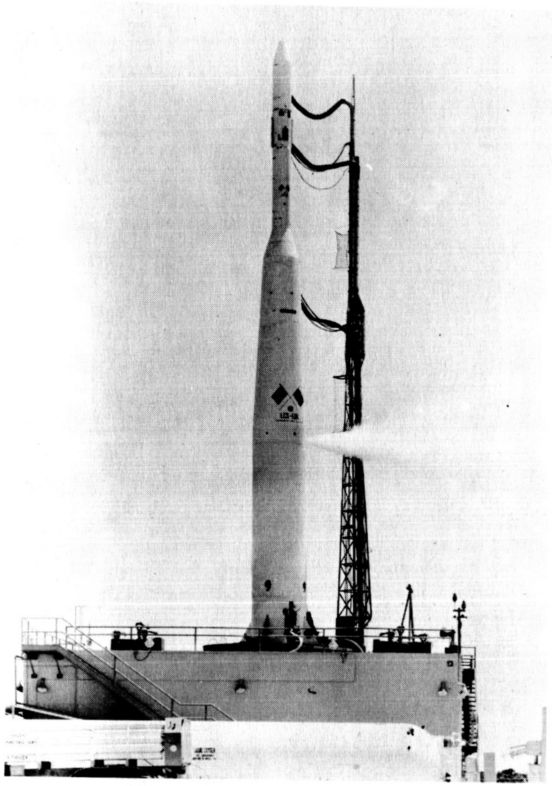

Figure 1—The Delta 9 vehicle on its launch pad at Cape Canaveral.

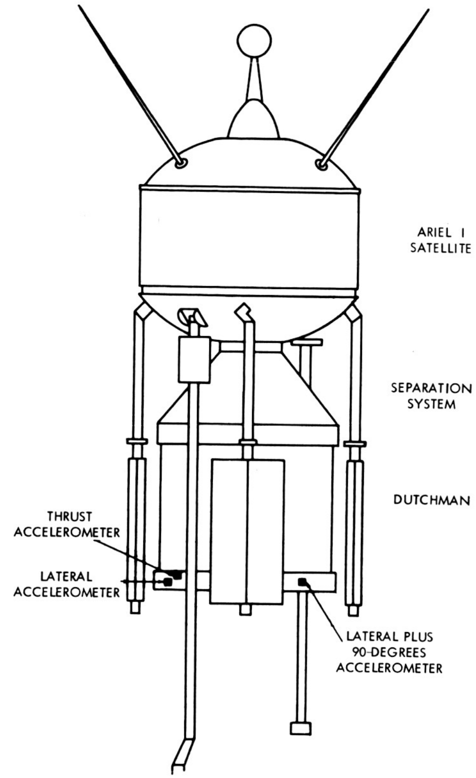

Figure 2—Locations of the accelerometers on the Dutchman.

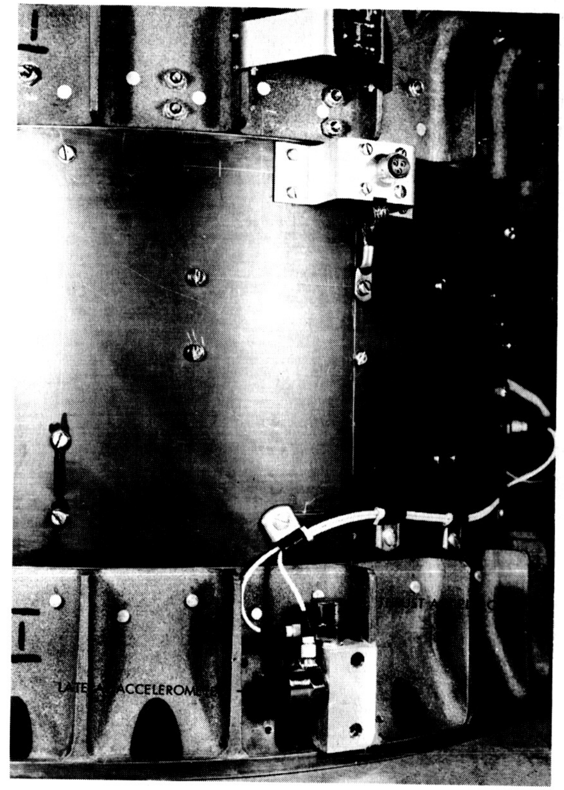

Figure 3—Locations of the thrust and lateral accelerometers on the Dutchman.

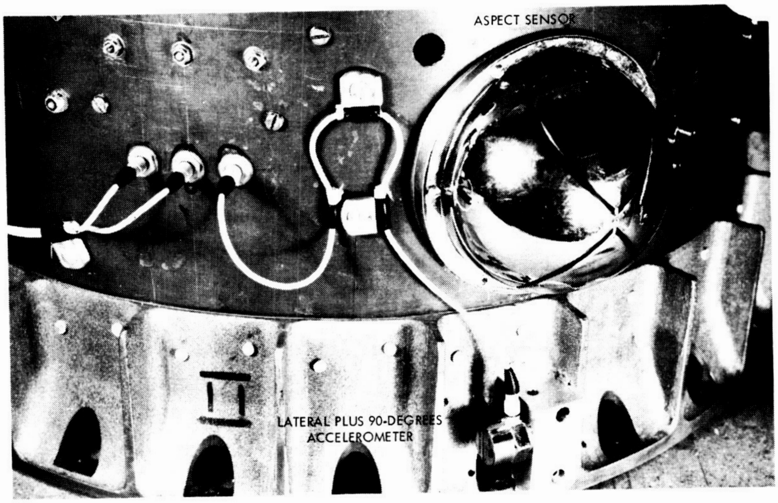

Figure 4—Locations of the lateral plus 90-degree accelerometer and the aspect sensor on the Dutchman.

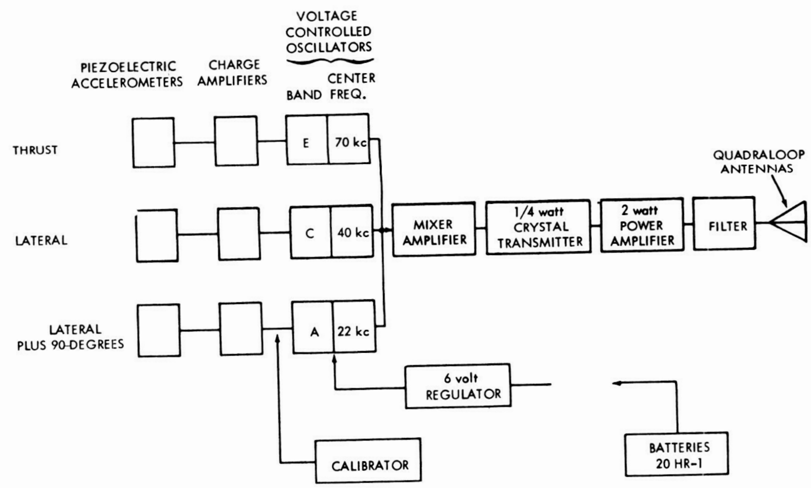

Figure 5—Instrumentation system.

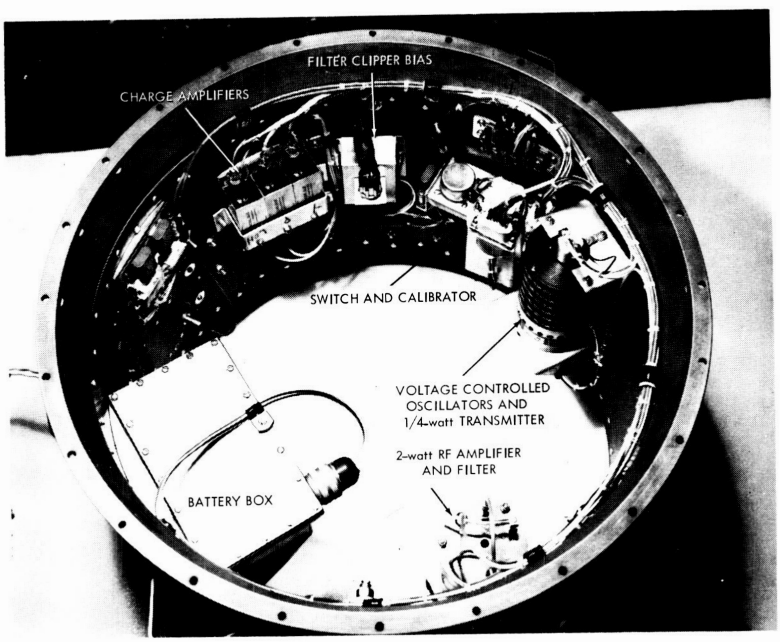

Figure 6—Vibration telemetry package.

increased to 5 kc without causing an increase in intermodulation distortion on other channels. The frequency response of the vibration instrumentation is shown on Figure 7 for the three telemeter channels. The thrust accelerometer had a range of ±50 g,the lateral and lateral plus 90-degree accelerometers had ranges of ±20 g. It is possible to measure vibration levels greater than those mentioned above before clipping the signal due to the low-rolloff RC low-pass filters.

DATA REDUCTION

A block diagram of the data reduction system is shown in Figure 8. Data reduction consisted of various oscillograph records, rms vibration time plots, and 1/3-octave band analysis.

RESULTS

For ready reference and information, the vehicle trajectory parameters and event times are presented in Table 1. The trajectory of Delta 9 was considered nominal, and all flight events occurred approximately at the predicted event time, except the time of the first despin sequence. Table 2 is a vibration data summary of the Delta 9 read from real-time oscillograph records.

The rms vibration time histories for the three axes are shown on Figure 9 during first- and second-stage burning. Vibration transients occurred at liftoff and first-stage engine cutoff along the three axes. Second-stage ignition transients are obscured, because of RF dropout. Transients also occurred along the two lateral axes when the fairing was jettisioned, and along all three axes at second-stage engine cutoff. Table 3 is a summary of the predominant frequencies and maximum levels of these transients. The vibration levels at times other than listed event times were less than 0.63 g rms and 0.25 g rms, in the thrust and lateral directions, respectively. There was no significant increase in vibration levels at either Mach 1 or Maximum Q.

Figure 10a displays the composite vibration along the thrust axis at liftoff of all frequencies below 1000 cps. The maximum peak level was 2.5 g. But, as shown on Figure 10b, the major vibration occurs at 16 cps. The maximum peak g level was 1.45. This level occurred at 0.25 sec after liftoff and decays to 0.3 g peak at T + 2 sec. Figure 10c depicts the 46.5 cps component during liftoff. The maximum level at this frequency was 1.07 g peak but was a single cycle. An average over a six-cycle period was 0.55 g peak.

The lateral axis liftoff transient essentially consists of two frequencies; 10.5 cps and 40 cps with maximum levels of 0.7 g peak and 0.66 g peak, respectively (see Figure 11). The lateral plus 90-degree axis liftoff transient (Figure 12) consists of the same frequencies as the lateral axis with levels of 0.4 g peak and 0.58 g peak for 10.5 cps and 40 cps, respectively. The results of an experimental modal analysis performed on a Transit/Tiros vehicle, similar in configuration to the Delta 9, indicated a second bending mode at 10.7 cps (Reference 2).

The data exhibited on Figure 13 show the presence of a 26 cps thrust axis resonance associated with this Thor vehicle. The resonance starts at T + 155 and lasts to main engine cutoff, that is,

(a) Thrust axis

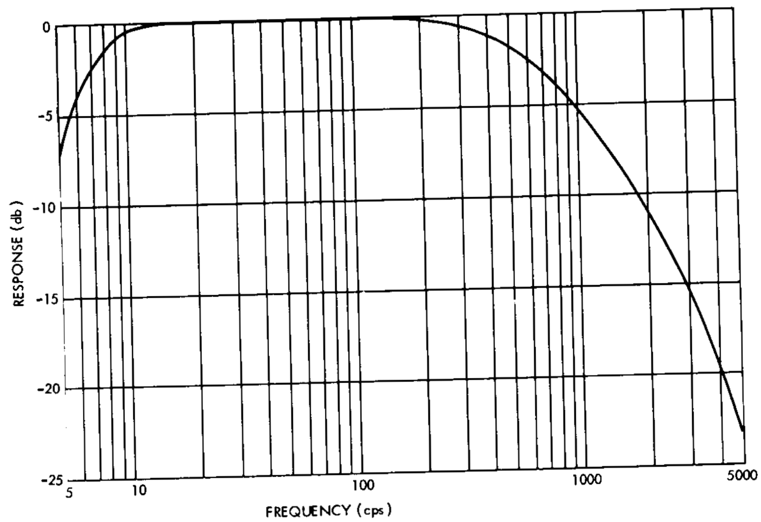

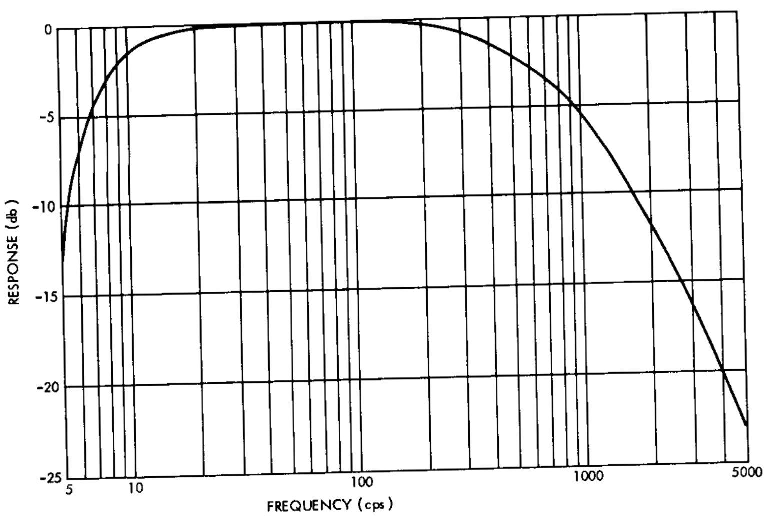

(b) Lateral axis

(c) Lateral plus
90-degree axis

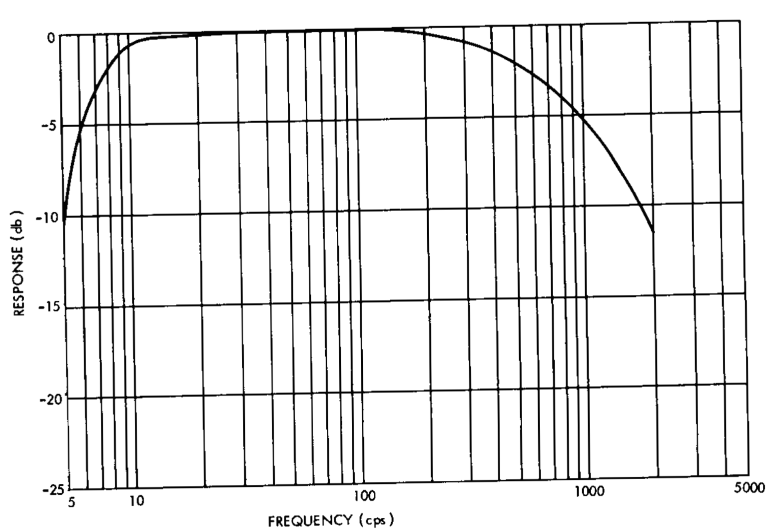

Figure 7—Frequency response of the vibration experiment and playback instrumentation.

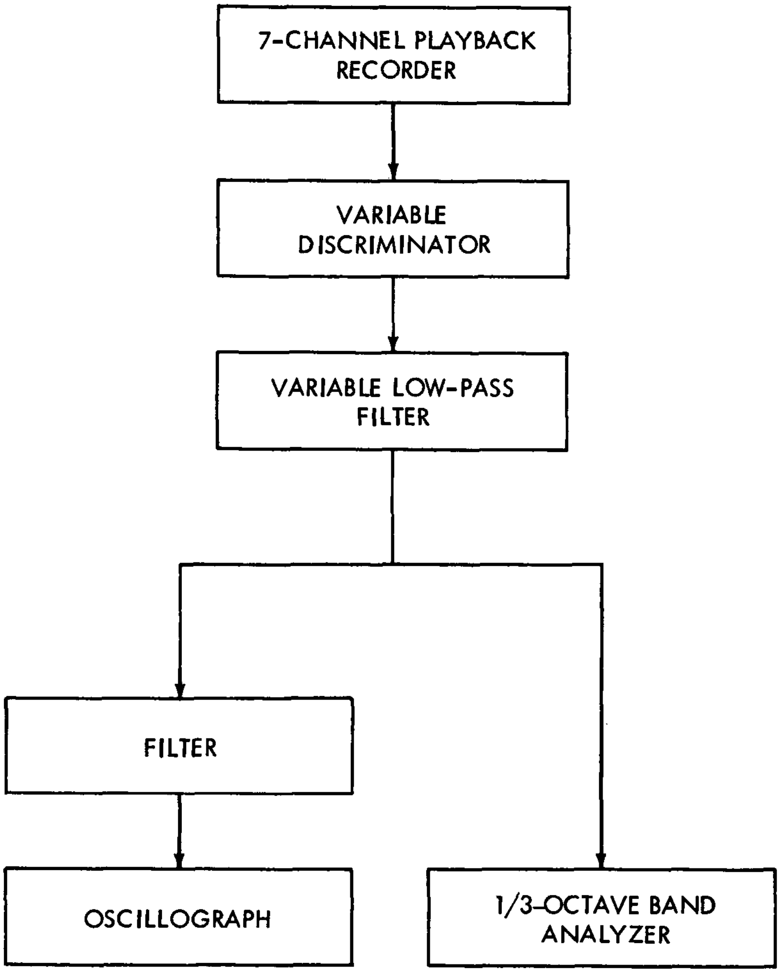

Figure 8—The data reduction systems.

Table 1

Delta 9 Vehicle Trajectory Parameters and Event Times.

Event	Time (sec)	Greenwich Mean Time (Zulu)	Altitude (n. mi.)	Relative Velocity (fps)
First-Stage Ignition	-3.5	--	0	--
Liftoff	0	1800:16.9	0	0
Mach I	*50	1801:06.9	--	1,100
Maximum Q	*66	1801:32.9	--	2,000
First-Stage Cutoff	159	1802:55.8	41.3	15,446
Second-Stage Ignition	163	1802:59.9	44.5	15,438
Fairing Jettison	194	1803:29.3	--	--
Second-Stage Cutoff	261	1804:37.9	103.8	20,619
Fire Spin Rockets	638	1810:55	--	--
Blow Separation Bolts	640	1810:57	--	--
Third-Stage Ignition	653	1811:10	213	19,638
Third-Stage Burnout	695	1811:52	212	24,955
Premature Despin				
1st	757	1812:54	--	--
2nd	767	1813:04	--	--
3rd	777	1813:14	--	--
4th	837	1814:14	--	--

*Calculated values, not actual flight data.

Table 2

Vibration Data Summary of the Delta 9 Vehicle.

Event	Composite Acceleration (peak g)		
	Thrust Axis	Lateral Axis	Lateral plus 90-Degree Axis
First-Stage Ignition	--	--	--
T-1	0.5	0.5	0.3
Liftoff, T + 0	2.50	1.9	0.9
Liftoff + 1 second	0.75	0.6	0.6
Main Engine Cutoff	2.0	0.3	0.4
Second-Stage Ignition	*	*	*
Jettison Fairing	0.25	1.0	1.0
Second-Engine Cutoff	2.25	0.3	0.3
Spinup	--	0.47	0.4
Blow Second-Third-Stage Separation Bolts	--	1.57	0.4
Third-Stage Ignition	†	†	†

*RF signal dropout.

†See Table 4 and the discussion on page 10.

T + 159, at which time elastic rebound is seen. This resonance dies out at T + 161. The frequency of this resonance was 26 cps with a maximum acceleration level of 1.47 g peak. At T + 160.3 the lateral plus 90-degree axis shows a level of 0.2 g peak at 26 cps. Figure 14 shows a 46.5 cps resonance in the thrust direction at main engine cutoff with an acceleration level of 0.95 g peak.

Figure 15a shows two transients that were measured along the lateral axis during fairing jettison. The two pulses occurred approximately 1 sec apart. The vibration level of the first transient was 0.88 g peak while the second transient's maximum level was 0.98 g peak at a

(a) Thrust axis. Low-pass output filter (4.2 kc).

(b) Lateral axis. Low-pass output filter (2.1 kc).

(c) Lateral plus 90-degree axis. Low-pass output filter (2.1 kc).

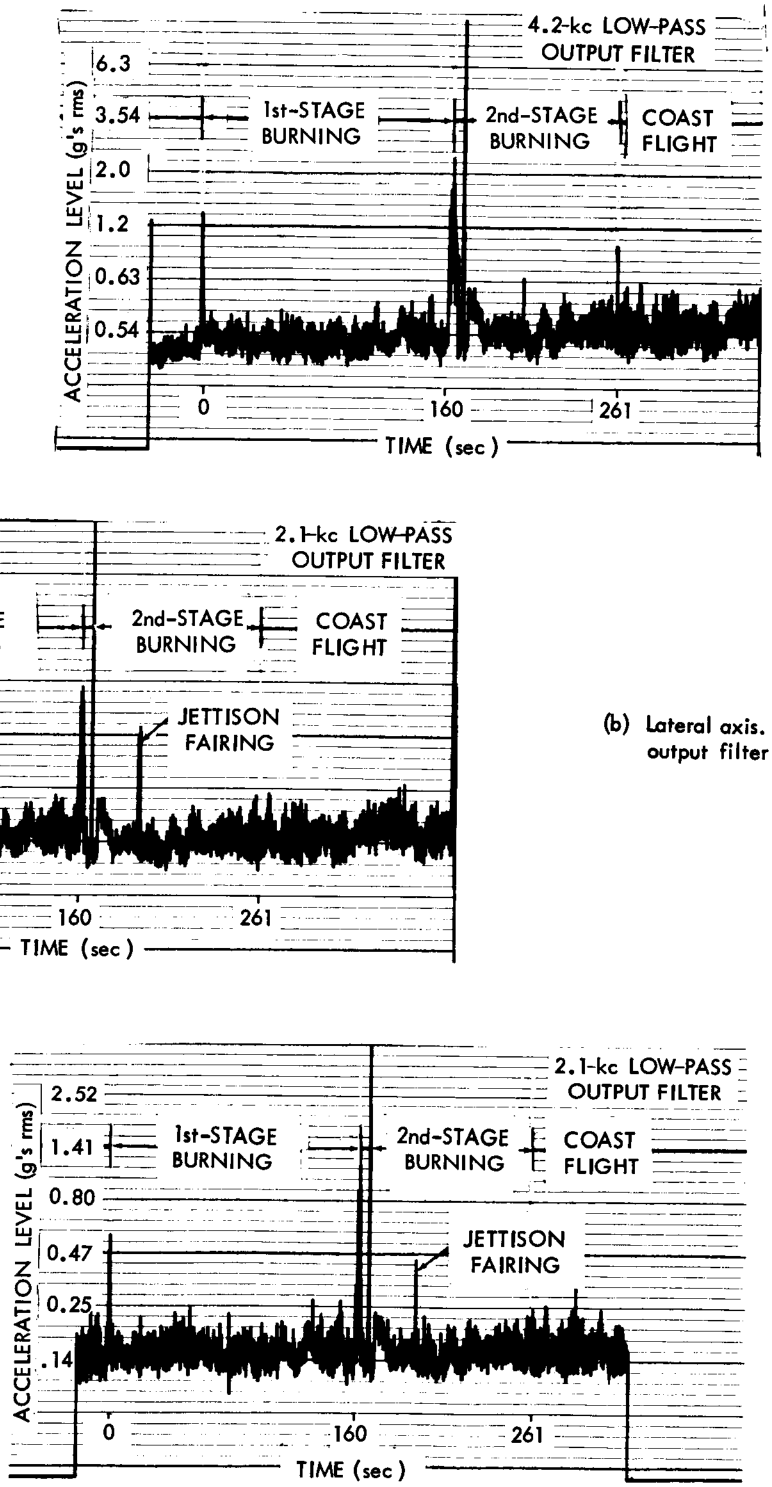

Figure 9—Vibration time history, composite of all frequencies. Pen speed 160 mm/sec, paper speed 0.3 mm/sec.

Table 3

Transient Component Analysis for the Delta 9 Vehicle: Predominant Frequencies and Maximum Levels.

Event	Thrust Axis		Lateral Axis		Lateral plus 90-Degree Axis	
	Peak Acceleration (g)	Frequency (cps)	Peak Acceleration (g)	Frequency (cps)	Peak Acceleration (g)	Frequency (cps)
Liftoff	1.45 1.07	16 46.5	0.7 0.66	10.5 40	0.4 0.58	10.5 40
First-Stage Cutoff	1.47 0.95	*26 46.5	-- --	-- --	0.2	26
Jettison Fairing	--	--	0.98	8	0.57 0.31	8.9 60
Second-Stage Cutoff	1.25	44	--	--	--	--
Second-Third-Stage Separation Bolts	--	--	1.57	9.4	--	--

*This frequency lasts for approximately 6 sec. The levels of all other frequencies decay to insignificant values within 3 sec.

frequency around 8 cps. Figure 15b depicts a component of the transient along the lateral plus 90-degree axis at approximately 9 cps with a level of 0.57 g peak. Figure 15c shows another component of the above transient at 60 cps with a level of 0.31 g peak.

Elastic rebound of the vehicle is noted at second-stage cutoff (Figure 16). The major component of this transient was 44 cps with a maximum level of 1.25 g peak. This transient decays to an insignificant level in 0.2 sec.

Figrue 17 depicts the major frequency component along the lateral axis of the transient that occurred during explosion of second- and third-stage separation bolts. The maximum level was 1.57 g peak at approximately 9.4 cps.

Figure 18 is an oscillograph record of uncorrected composite vibration levels during third-stage burning. A high percentage of the data shown on the record for the two lateral axes are erroneous.

The distorted shapes of the oscillograph traces are attributed to charge amplifier overload caused by high-level input signals. The accelerometer systems were set up to measure low-level first- and second-stage motor excitations. It was known that the electronic systems would probably be overloaded during third-stage motor burning, but other data are available on this type of motor, that is, from Scout vehicle flights. However, some data for the thrust axis are valid. Since, at the present time, no tracking analyzer is available to lock onto the sliding tones that occurred during third-stage burning, a 1/3-octave band analysis was made on the thrust axis vibration. These tones slide at a rate of approximately 100 cps/sec. With two exceptions, vibration levels in the bands were corrected for system frequency response by applying the correction for the center frequency of that

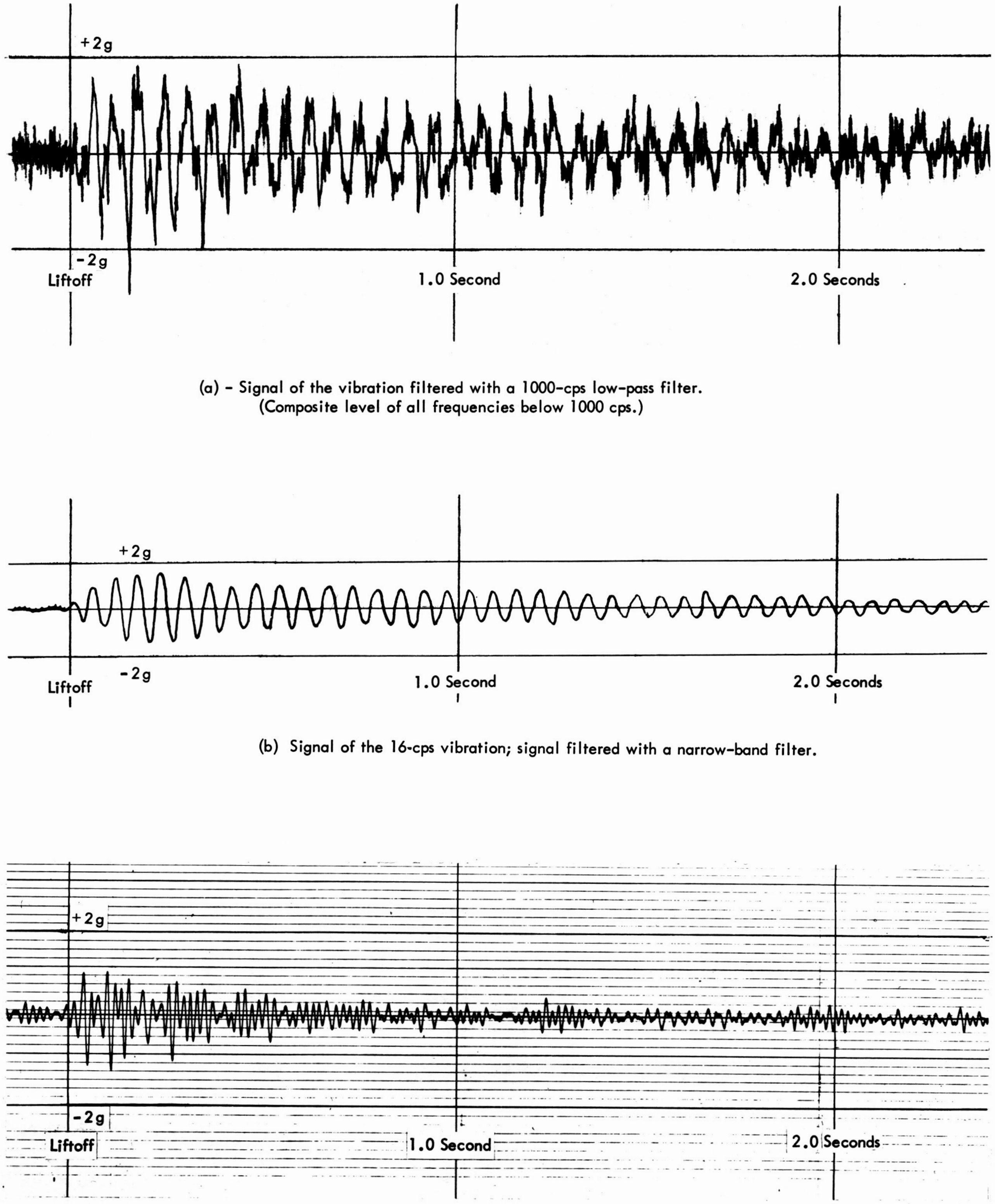

(a) - Signal of the vibration filtered with a 1000-cps low-pass filter.
(Composite level of all frequencies below 1000 cps.)

(b) Signal of the 16-cps vibration; signal filtered with a narrow-band filter.

(c) Signal of the 46.5-cps vibration; signal filtered with a narrow-band filter.

Figure 10—Thrust axis vibration at liftoff; instantaneous acceleration versus time.

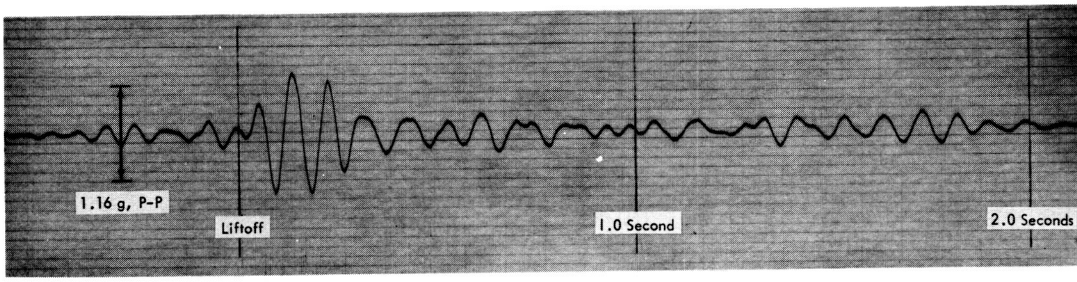

(a) Signal of the 10.5-cps vibration.

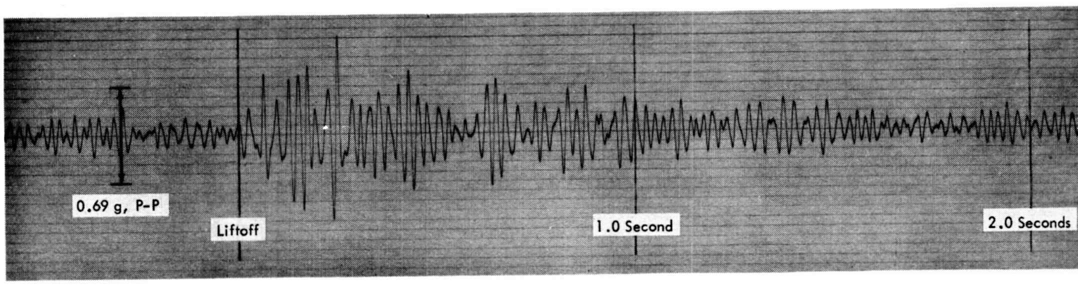

(b) Signal of 40-cps vibration.

Figure 11—Lateral axis vibration at liftoff; instantaneous acceleration versus time; signals filtered with a narrow-band filter.

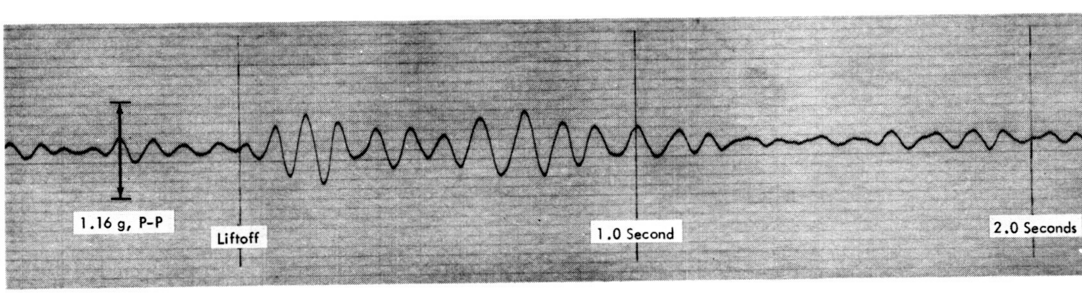

(a) Signal of the 10.5-cps vibration.

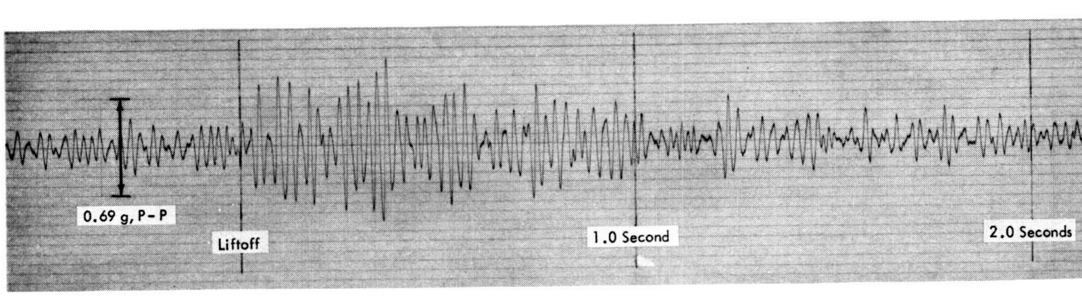

(b) Signal of the 40-cps vibration.

Figure 12—Lateral plus 90-degree axis at liftoff; instantaneous acceleration versus time; signals filtered with a narrow-band filter.

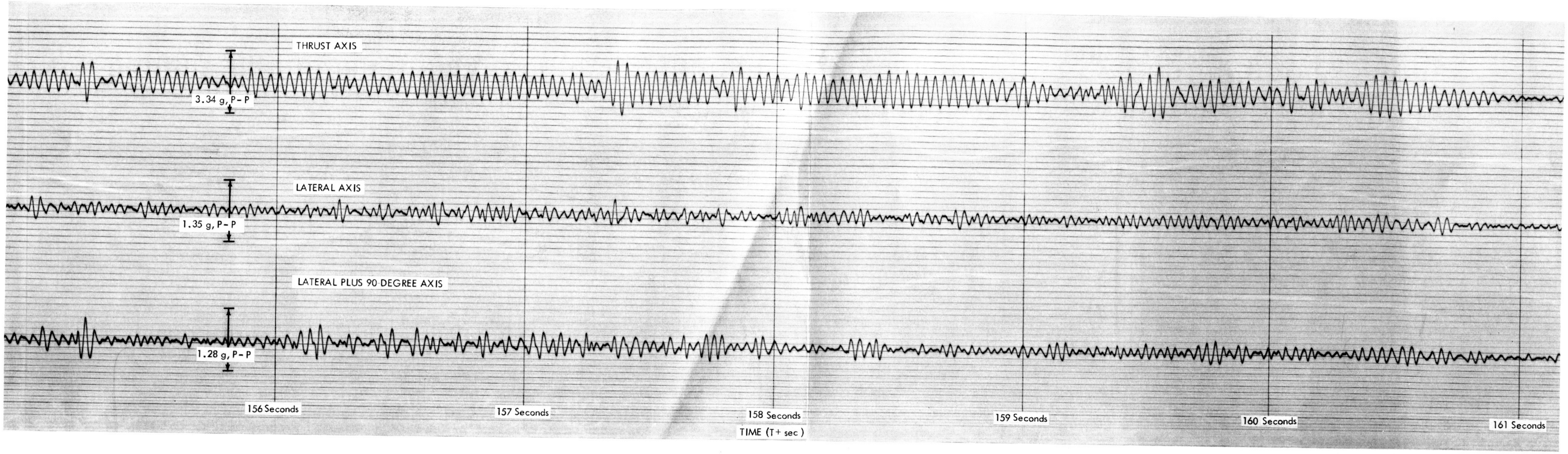

Figure 13—Vibrations at first-stage engine cutoff; instantaneous acceleration versus time; signal filtered with a narrow-band filter. Signal of the 26-cps vibration.

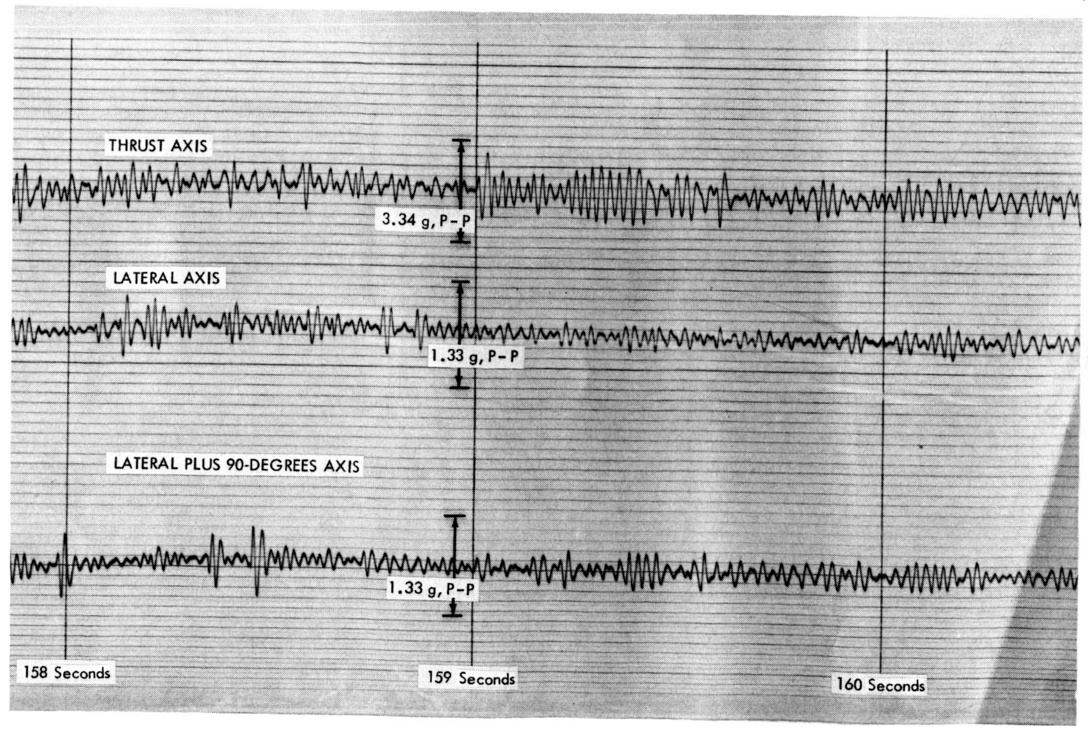

Figure 14—Vibrations at first-stage engine cutoff; instantaneous acceleration versus time; signal filtered with a narrow-band filter. Signal of the 46.5-cps vibration.

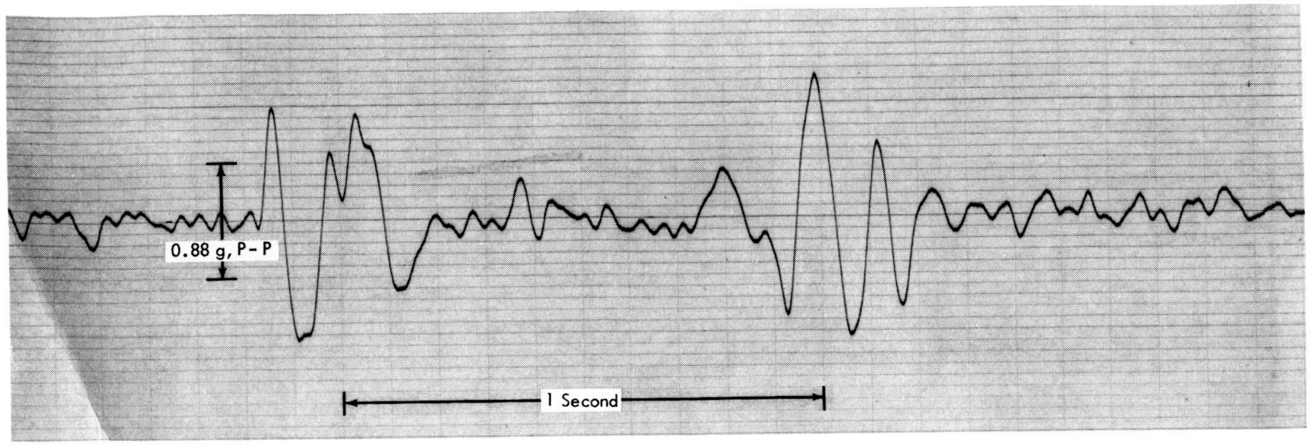

(a) Lateral axis. Signal of the 8-cps vibration.

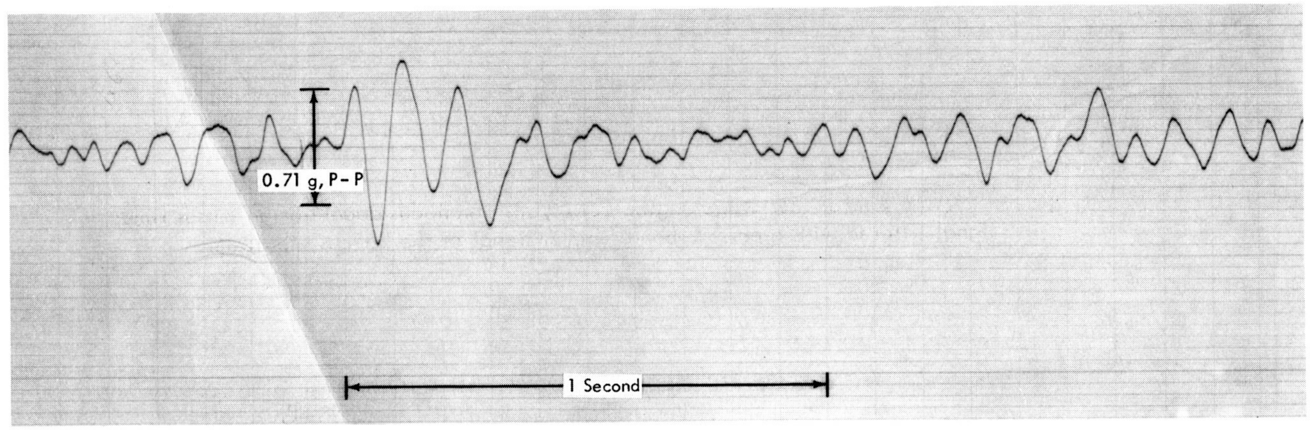

(b) Lateral plus 90-degree axis. Signal of the 9-cps vibration.

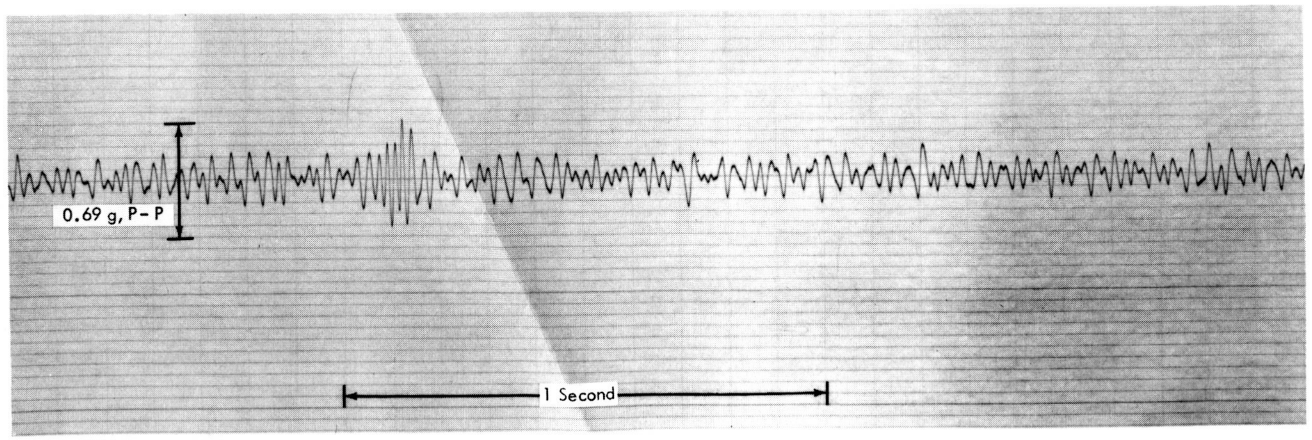

(c) Lateral plus 90-degree axis. Signal of the 60-cps vibration.

Figure 15—Vibration at fairing jettison; instantaneous acceleration versus time; signals filtered with a narrow-band filter.

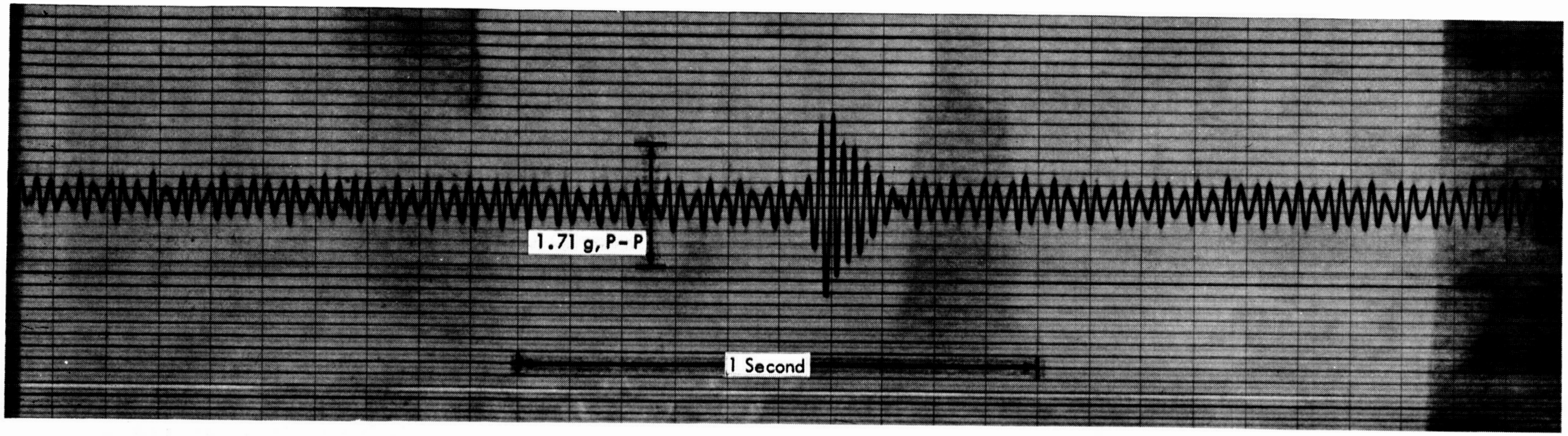

Figure 16—Thrust axis vibration at second-stage engine cutoff; instantaneous acceleration versus time; signal filtered with a narrow-band filter. Signal of the 44-cps vibration.

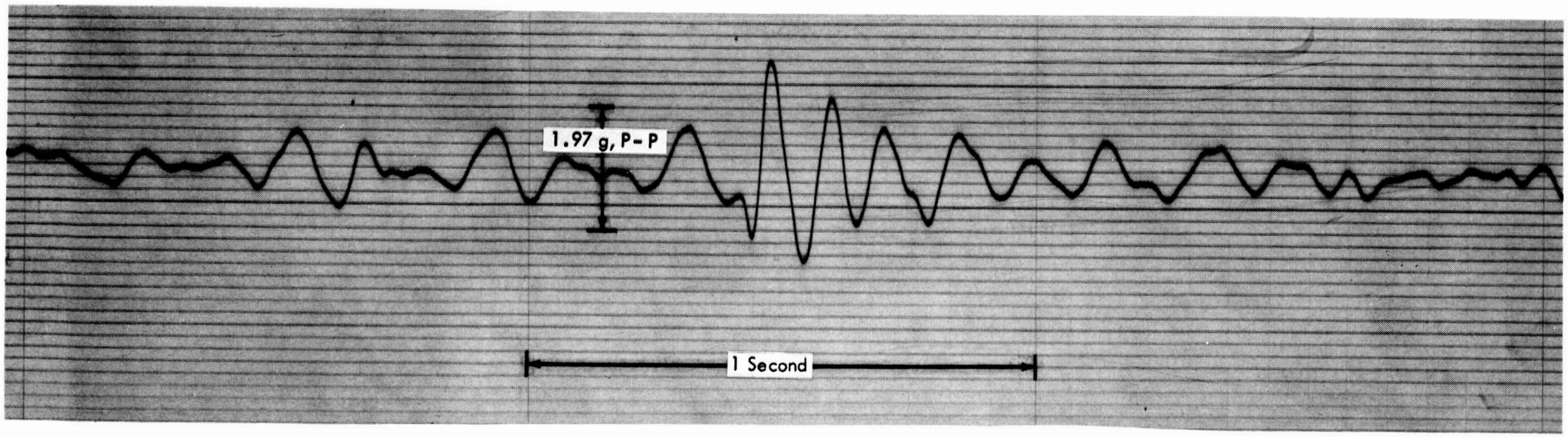

Figure 17—Lateral axis vibration at second- and third-stage separation; instantaneous acceleration versus time; signal filtered with a narrow-band filter. Signal of the 9.4-cps vibration.

Table 4

Delta 9 Third-Stage Vibratory Acceleration Measured Along the Thrust Axis During Third-Stage Burning

One-third-octave band analysis. All entries corrected for frequency response; paper speed 10 mm/sec; pen writing speed 160 mm/sec; low-pass output filter (4200 cps).

Center Freq. (cps)	Ign t=0	MAXIMUM ACCELERATION (g rms) AT TIME t (sec)																
		t=1	2	3	4	5	6	7	8	9	10	11	12	13	14	15	16	17
40							.4			.13								.2
50						.16	.22			.2			.14					
63	.18									.18								
80	.16									.18								
100	.16						.14	.13		.16								
125	.18				.16	.13			.16	.18								
160	.16			.16	.16		.16		.14	.22		.22						
200	.14		.13	.16	.2		.25	.2	.18	.2	.2	.16						
250	.16	.16	.16	.16	.19	.26	.27	.2	.2	.30	.16	.16	.16	.14	.14	.16	.19	.19
320	.30	.32	.40	.30	.30	.61	.54	.37	.34	.38	.25	.28	.28	.28	.30	.28	.29	.32
400	.16	.20	.22	.20	.25	.25	.28	.22	.25	.25	.22	.20	.19	.16	.15	.16	2.08	2.08
500	.22		.17		.22				.22	.27			.19				.68	.68
630	.30	.30	.19	.19	.25		.25	.30	.26	.28	.22							
800	.35				.30	.24			.31	.33			.60					
1K	.32				.32	.57			.32	.33			.85				.24	
1250	.44				.40	.35			.40	.40	.38						.28	.40
1600	.79				.50		.40		.56	.56	.44		1.12	.35	.40	.50	.71	.71
2K	.71	.44	.44	.44	.71	.50	.56	.56	.71	.71	.79	.50	1.58	2.24	3.96	7.06	9.95	11.2
2.5K	2.5	.79	.79	.89	1.25	1.25	1.41	1.58	3.15	4.6	3.54	1.41	35.4	39.7	56.1	56.1	56.1	46.5
3.2K	2.5	3.5	5.0	7.9	17.7	21.8	21.8	12.5	12.5	12.5	11.0	11.0	8.8	7.9	5.6	5.6	4.4	3.5
4K	28.8	26.5	25.0	25.0	15.8	8.9	6.0	4.0	4.8	5.6	5.6	4.0	16.0	4.4	4.4	3.5	4.4	6.3
5K													← OVERLOAD →					

Center Freq. (cps)	MAXIMUM ACCELERATION (g rms) AT TIME t (sec)																			
	18	19	20	21	22	23	24	25	26	27	28	29	30	31	32	33	34	35	36	37
40																				
50																				
63																				
80																				
100																				
125																				
160	.13																		.14	
200	.16														.14	.13				
250	.23	.16	.16	.16	.18	.16	.18	.16	.16	.16	.17	.13	.14	.16	.16	.16	.13			
320	.43	.38	.38	.38	.43	.38	.45	.43	.43	.45	.43	.32	.34	.34	.34	.34	.32	.30	.38	.34
400	.25	.20	.22	.25	.25	.25	.25	.22	.20	.23	.23	.16	.23	.20	.22	.25	.22	.20	.22	.20
500	.22		3.9	3.9	3.9	3.9	3.9	3.7	3.0	2.5	1.3	.49	.49		.24	.43				
630	.25		13.4	13.4	13.4	12.0	10.7	9.6	7.6	5.9	2.5	1.1	.54	.27	.27	.43				
800	.31		.54	.54	.54	.52	.48	.39	.31	.26										
1K	.32		.24	.24																
1250	.56	.28	.71	.79	.63	.50	.44	.35	.32	.32										
1600	.56			.40	.40	.44	.44	.44	.40	.40										
2K	4.0	.50	.56	.56	.50	.44	.56	.56		.56	.50			.56			.44	.44		
2.5K	7.9	.89	1.41	.89	.79	.79	.79	.79	.79	.79	.79	.79	.83	.56	.79	.71	.71	.71		
3.2K	3.5	2.0	3.2	1.8	1.7	1.6	1.4	1.4	1.6	1.4	1.4	1.4	1.4	1.4	1.4	1.4	1.2			
4K	7.0	4.0	4.0	3.5																
5K																				

Figure 18—Composite uncorrected vibration levels of the third-stage motor; instantaneous acceleration versus time.

particular band as shown on Figure 7. The two exceptions are: the corrections in the center frequency (CF) bands 400 cps and 630 cps were taken at 450 cps and 580 cps, respectively, since these are constant frequency vibration. The results of the analysis are shown in Table 4.

A longitudinal resonant burning mode of the X-248 started 20 sec after motor ignition. The frequency of this oscillation was 577 cps. The vibratory level increased quickly to 13.4 g rms and in 10 sec had gradually decreased to 0.54 g rms. The level in the lateral plus 90-degree axis was 1.58 g rms at the start of this mode then gradually decreased with increased burn time.

The longitudinal vibrations (sliding tones) begin at ignition at frequencies in the 4-kc CF band and slide down to frequencies in the 2-kc CF band 17 sec later. These vibrations (sliding tones) reached a maximum level (56.1 g rms) 14 sec after ignition in the 2.5-kc CF band. This level is not realistic, since the charge amplifiers would be overloaded at this level (see Table 4).

Shock transients that occurred during premature despin of the third-stage motor-payload combination are shown on Figure 19. The despin sequence was scheduled to start 15 minutes after third-stage pressure switch closure. However, the first despin occurred 1 min and 40 sec after switch closure. At this time the rocket-payload despun from 158 ± 2 rpm to 122 ± 2 rpm in a few tenths of a second. Ten seconds later it despun to 103 ± 2 rpm and 20 sec after initial despin the spin rate dropped to 90 ± 2 rpm. There was no visible shock transient on the oscillograph record at 90 rpm. Another minute later it again despun to 78 ± 2 rpm. The despins were caused by premature erection of booms and paddles.

DISCUSSION

No significant increase in vibration levels was noted during times of Mach 1 or Maximum Q. This is attributed to the streamlined design of the vehicle which greatly reduced buffeting, and to the mode of connection of the Delta 9 fairing. This vehicle used a low-drag fairing (bullet shaped) and not a bulbous one, and connects to the second-stage vehicle. All fairing vibration would be attenuated by the third-stage dynamics.

Three of the premature despin events of the third-stage vehicle were accompanied by short duration shocks which occurred when booms and paddles snapped into erected positions. The spin reduction was in these cases completed in about 0.5 sec, and it is clear from the records that the reduction was completed by the time that the shocks occurred. This is consistent with boom erection rather than the exertion of external impulses (as from motor "chuffing") where the despin accompanies the impulse. For the fourth despin there was no shock transient and the duration of the despin was slightly greater (A. P. Willmore, private communication).

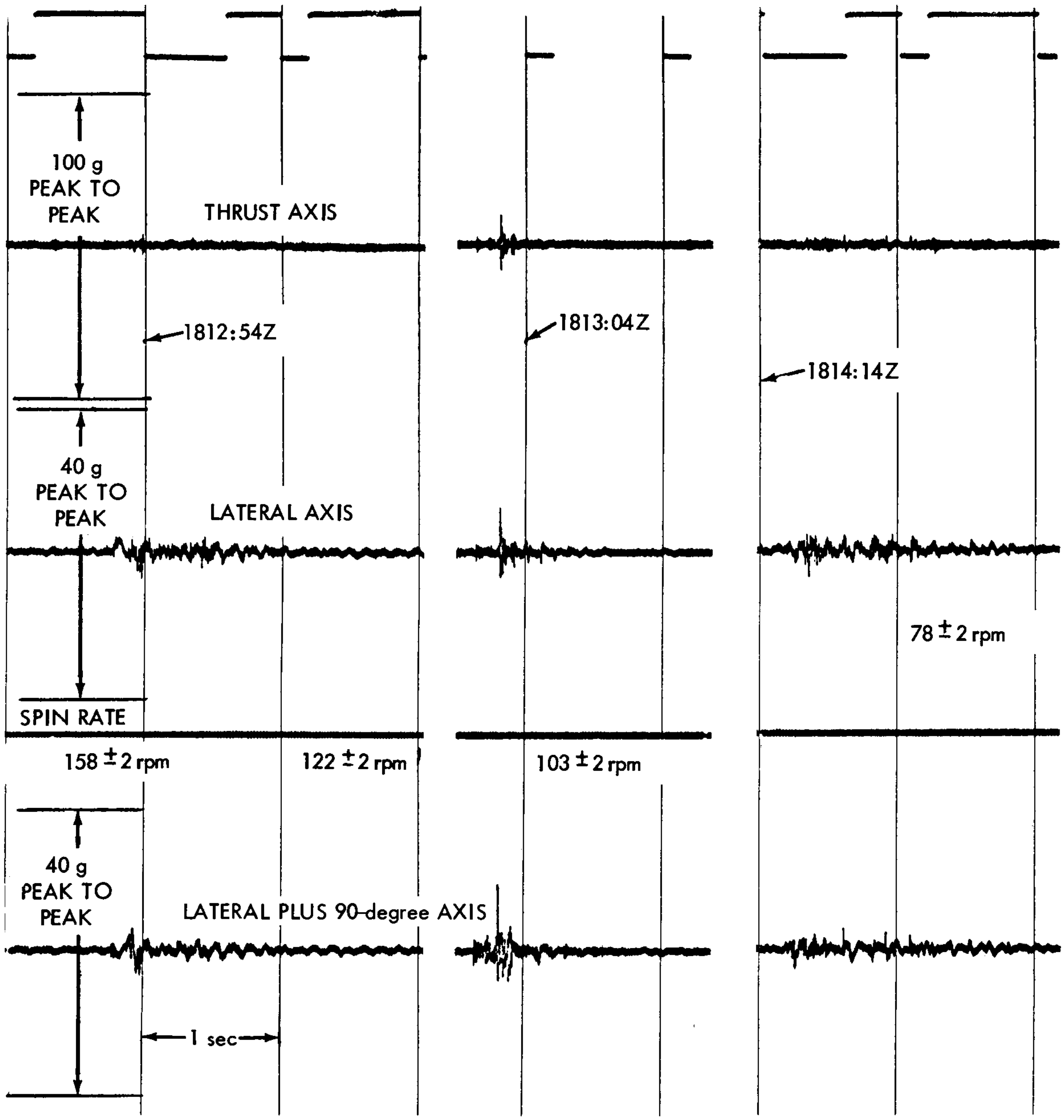

Figure 19—Vibration levels at premature despin; instantaneous acceleration versus time.

REFERENCES

1. Flight Report for Vehicle 320/2019/3019, Delta Program - Mission No. 9 S-51 Spacecraft, Douglas Aircraft Company, Report SM-41911, June 1962.

2. Engineering Test Report - Model DM 1812-2, Vibration Test - Transit/Tiros Body Bending Modes, Douglas Aircraft Company, Tulsa Division Report TU-24534, June 16, 1960.

NASA-Langley, 1963 G-344